PHYSICAL REVIEW D **85,** 067301 (2012)

Standard big bang nucleosynthesis with a nonthermal reaction network

Victor T. Voronchev,[1] Yasuyuki Nakao,[2] Kazuki Tsukida,[2] and Makoto Nakamura[3]

[1]*Institute of Nuclear Physics, Moscow State University, Moscow 119991, Russia*

[2]*Department of Applied Quantum Physics and Nuclear Engineering, Kyushu University, Motooka, Fukuoka 819-0395, Japan*

[3]*Division of Advanced Plasma Research, Japan Atomic Energy Agency, 2-166 Oaza-Obuchi-Aza-Omotedate, Rokkasho, Kamikita, Aomori 039-3212, Japan*

(Received 3 December 2011; revised manuscript received 25 January 2012; published 9 March 2012)

We discuss a refined scenario of standard big bang nucleosynthesis (BBN) allowing for nonthermal nuclear reactions in the primordial plasma. These reactions are naturally triggered in the early Universe by fast particles (n, p, t, ^{3}He, α) generated in the $t(d,n)\alpha$, $d(d,n)^3$He, $d(d,p)t$, and ^{3}He$(d,p)\alpha$ processes. We take into account the nonthermal channels for reactions between nuclei with $A \leqslant 7$ (of the standard BBN network) and consider new processes, such as nucleon-induced breakups of fragile d, ^{6,7}Li, and ^{7}Be. It is shown that fast neutrons—the most abundant and hot nonthermal plasma species—can effectively maintain some reactions as the Universe cools. Depending on the type of an individual reaction, these neutrons can increase the reaction rate coefficient $N_A\langle\sigma v\rangle$ by a few percent (for exoergic resonant processes) and orders of magnitude (for endoergic processes, such as the breakups and some reverse reactions). However, the individual nonthermal effects prove to be insufficient to influence the whole reaction kinetics and significantly change the predictions of thermal BBN. The nonthermal corrections to element abundances are found to be 0.10% (for T), -0.01% (for ^{3}He), -0.02% (for ^{7}Li), and 0.36%–0.60% (for CNO elements).

DOI: 10.1103/PhysRevD.85.067301 PACS numbers: 26.35.+c, 95.30.$-$k

I. INTRODUCTION

Big bang nucleosynthesis (BBN) plays a central role in the hot cosmology and remains the most reliable probe of the early Universe physics. A degree of agreement between abundances of light elements predicted theoretically and those inferred from observations reflects our understanding of processes in the primordial plasma. The standard model of BBN (SBBN) [1,2], being a parameter-free theory since the first release of WMAP data [3], provides a remarkable approach to describe the early Universe evolution. It has been recognized that SBBN, with the WMAP's baryon density, gives good predictions for the abundances of primordial D and ^{4}He but appreciably overestimates the amount of primordial ^{7}Li by a factor of 3–4. A reason for this discrepancy has still not been understood. It may come from errors in observational data and their treatment, insufficient accuracy of SBBN outputs, or even reflect a signature of new physics beyond the standard model. For details, we refer the reader to recent reviews [4–8] and references therein.

In view of this, the accuracy of SBBN predictions is a crucial issue which must be well realized. Being essentially dependent on some input data, SBBN predictions have been updated whenever revised major inputs (fundamental constants, reaction rate parameters, etc.) become available in the literature. At the same time, new reactions as well as specific plasma effects and related reaction peculiarities have been extensively investigated. Note here some of the most recent works: A significant extension of BBN calculations up to CNO by adding a large number of new processes for particles with mass number $A \leqslant 20$ was reported in [9,10]. New reactions for ^{3}He–^{3}H, ^{7}Li–^{7}Be, and ^{9}Be nuclei and their influence on element abundances were analyzed in [11]. Specific phenomena were studied in [12] (independent neutrino distributions), [11] (thermal excitation of nuclei), [13] (screening of subbarrier reactions), etc. Resonant destruction of $A = 7$ isotopes as a possible mechanism to alleviated the ^{7}Li discrepancy was discussed in [14,15].

There still remains an issue which has not been studied in detail. As is known, SBBN relies on the reaction network operating with thermal equilibrium processes. At the same time, however, some nonthermal processes can also occur in the early Universe. The most natural ones are in-flight reactions induced by energetic particles during slowing down in the plasma [11,16–19]. These particles are predominantly produced in the $t(d,n)\alpha$, $d(d,n)^3$He, $d(d,p)t$, and ^{3}He$(d,p)\alpha$ fusion reactions and may be considered as primordial isotropic "cosmic rays." They form groups of non-Maxwellian species (n, p, t, ^{3}He, α) which perturb the respective particle distribution functions so that their high-energy tails deviate from a Maxwellian function.

In preceding papers [18,20] we examined the formation and properties of these groups and demonstrated their influence on some reactions. Our present goal is to incorporate nonthermal reactions in the BBN network [21,22] and realize whether they can affect reaction kinetics and change the primordial element production. In other words, the purpose is to generalize SBBN by taking into account non-Maxwellian nuclear processes naturally occurring in the early Universe.

II. NONTHERMAL PHENOMENA AND ELEMENT ABUNDANCES

First of all, it is worthwhile to summarize main characteristics of the nonthermal particle groups $l(= n, p, t, {}^3\mathrm{He}, \alpha)$. Based on results [18,20], this is done in Table I. A combination of high emission rate and comparatively low energy loss makes $t(d, n)\alpha$ and $d(d, n)^3\mathrm{He}$ fusion neutrons the most abundant and hot nonthermal plasma species. Their number density and effective temperature essentially exceed those for charged particles c. The most hot c-group is formed by $3\mathrm{He}(d, p)\alpha$ protons, but their fraction in primordial hydrogen is very small. It is important that all these particles can enhance some "standard" reactions and activate new (endoergic) processes.

To run extended SBBN simulations allowing for nonthermal effects, we have generalized the standard code [22] so as to incorporate nonthermal forward and reverse processes in chain reaction kinetics. These processes are listed in Table II. The group Standard presents the nonthermal channels for reactions of the standard network [22] involving nuclei with $A \leqslant 7$ [23]. The group New gives reactions added to the network, such as two-body breakups of loosely bound nuclei $X(= d, {}^{6,7}\mathrm{Li}, {}^7\mathrm{Be})$ induced by fast nucleons.

TABLE I. Characteristics of nonthermal particles l generated in fusion reactions in the primordial plasma.

Particle	Reaction	$E_{l,0}$(MeV)[a]	R_l(cm^{-3} s^{-1})[b]	$\tau_{l,\mathrm{th}}$ (s)[c]	$\eta_{l,\mathrm{fast}}$[d]		$T_{l,\mathrm{fast}}$ (MeV)[e]
n	$t(d, n)\alpha$	14.07	9×10^{-15}	10^{-5}–10^{-1}	10^{-4}		5
n	$d(d, n)^3\mathrm{He}$	2.45	5×10^{-15}	10^{-5}–10^{-1}			
p	$^3\mathrm{He}(d, p)\alpha$	14.68	4×10^{-13}	10^{-11}–10^{-2}	6×10^{-16}	9×10^{-14}	2.14
p	$d(d, p)t$	3.02	4×10^{-15}	10^{-11}–10^{-2}	4×10^{-14}	4×10^{-14}	0.62
t	$d(d, p)t$	1.01	4×10^{-15}	10^{-11}–10^{-2}	1×10^{-9}	5×10^{-7}	0.34
^{3}He	$d(d, n)^3\mathrm{He}$	0.82	5×10^{-15}	10^{-12}–10^{-3}	2×10^{-8}	1×10^{-9}	0.28
α	$t(d, n)\alpha$	3.52	9×10^{-15}	10^{-11}–10^{-3}	4×10^{-12}	5×10^{-13}	0.97
α	$^3\mathrm{He}(d, p)\alpha$	3.67	4×10^{-13}	10^{-11}–10^{-3}	9×10^{-15}	4×10^{-13}	1.00

[a]Particle birth energy in the center-of-mass frame.
[b]Particle emission rate $R_l(T_9)$ has a single-peaked structure with maximum at $T_9 = 0.8$–0.9; shown is its peak value.
[c]Particle thermalization time $\tau_{l,\mathrm{th}}$ as the Universe cools from $T_9 = 1.22$ down to 0.08.
[d]Neutrons: fast neutron fraction $\eta_{n,\mathrm{fast}}(T_9) = n_{n,\mathrm{fast}}/n_n$ has a steplike form; shown is its average plateau value allowing for $t(d, n)\alpha$ and $d(d, n)^3\mathrm{He}$ fusion neutrons. Charged particles: $\eta_{c,\mathrm{fast}}(T_9)$ has a double-peaked structure with maxima at $T_9 = 0.81$–0.88 and 0.24; shown are the "hot" (left) and "cold" (right) peak values.
[e]Neutrons: fast neutron temperature $T_{n,\mathrm{fast}}(T_9)$ smoothly decreases as the Universe cools; shown is its average value allowing for $t(d, n)\alpha$ and $d(d, n)^3\mathrm{He}$ fusion neutrons. Charged particles: $T_{c,\mathrm{fast}}(T_9)$ has a single-peaked structure with maximum at $T_9 = 0.14$; shown is its peak value.

TABLE II. Nonthermal forward (f) and reverse (r) reactions induced by fast particles $(n, p, t, {}^3\mathrm{He}, \alpha)$.

No.	Reaction	Q(MeV)		No.	Reaction	Q(MeV)	
	Standard						
1	$p(n, \gamma)d$	2.22	f	17	$^7\mathrm{Li}(n, \gamma)^8\mathrm{Li}$	2.03	f
2	$d(p, \gamma)^3\mathrm{He}$	5.49	f	18	$^7\mathrm{Be}(p, \gamma)^8\mathrm{B}$	0.14	f
3	$d(d, n)^3\mathrm{He}$	3.27	r	19	$^7\mathrm{Be}(n, \alpha)\alpha$	18.99	f
4	$d(d, p)t$	4.03	r	20	$d(\alpha, \gamma)^6\mathrm{Li}$	1.47	f
5	$t(d, n)\alpha$	17.59	f	21	$^6\mathrm{Li}(p, \alpha)^3\mathrm{He}$	4.02	f
6	$^3\mathrm{He}(n, p)t$	0.76	f,r	22	$^6\mathrm{Li}(n, \alpha)t$	4.78	f
7	$^3\mathrm{He}(d, p)\alpha$	18.35	f	23	$^6\mathrm{Li}(p, \gamma)^7\mathrm{Be}$	5.61	f
8	$t(\alpha, \gamma)^7\mathrm{Li}$	2.47	f	24	$^6\mathrm{Li}(n, \gamma)^7\mathrm{Li}$	7.25	f
9	$^3\mathrm{He}(\alpha, \gamma)^7\mathrm{Be}$	1.59	f	25	$^6\mathrm{Li}(\alpha, \gamma)^{10}\mathrm{B}$	4.46	f
10	$^7\mathrm{Li}(p, \alpha)\alpha$	17.35	f	26	$^7\mathrm{Li}(\alpha, \gamma)^{11}\mathrm{B}$	8.66	f
11	$^7\mathrm{Be}(n, p)^7\mathrm{Li}$	1.64	f,r	27	$^7\mathrm{Be}(\alpha, \gamma)^{11}\mathrm{C}$	7.54	f
12	$d(n, \gamma)t$	6.26	f	New ($N = n, p$)			
13	$t(p, \gamma)\alpha$	19.81	f	28	$d(N, Nn)p$	-2.22	f
14	$t(t, 2n)\alpha$	11.33	f	29	$^6\mathrm{Li}(N, Nd)\alpha$	-1.47	f
15	$^3\mathrm{He}(n, \gamma)\alpha$	20.58	f	30	$^7\mathrm{Li}(N, Nt)\alpha$	-2.47	f
16	$^3\mathrm{He}(^3\mathrm{He}, 2p)\alpha$	12.86	f	31	$^7\mathrm{Be}(N, N^3\mathrm{He})\alpha$	-1.59	f

We employ two methods to treat nonthermal reactions. The first one is based on a formalism of in-flight reaction probability. According to it, the effective rate parameter of in-flight reactions between fast particles l and background species X is

$$\langle\sigma v\rangle_{lX,\mathrm{in-fl}} = \frac{1}{n_{l,\mathrm{fast}} n_X} R_l P_{lX}(E_{l,0} \to E_{\mathrm{th}}), \qquad (1)$$

where R_l and $n_{l,\mathrm{fast}}$ are the fast particle emission rate and number density, respectively, n_X is the target number density. The quantity P_{lX} is the probability for a particle l to undergo the $l + X$ reaction, while slowing in the plasma from an initial energy $E_{l,0}$ down to the thermal energy E_{th} [18]. We remind that the particle thermalization times are much shorter than a typical time scale of plasma evolution in the BBN epoch. Therefore, the plasma temperature and density can be assumed to "freeze out" during the time needed for the nonthermal reactions to proceed. The in-flight reactivity $\langle\sigma v\rangle_{lX,\mathrm{in-fl}}$ in a combination with the Maxwellian one $\langle\sigma v\rangle_{lX,\mathrm{M}}$ can be used to describe the nonthermal and thermal reaction channels. We apply this approach to charged-particle reactions.

The second method operates with distribution functions of reacting particles. In this case, the $l + X$ reactivity allowing for nonthermal and thermal components is calculated straightforwardly

$$\langle\sigma v\rangle_{lX} = \frac{1}{n_l n_X} \int f_l(\mathbf{v}_l) f_X(\mathbf{v}_X) \sigma_{lX} |\mathbf{v}_l - \mathbf{v}_X| d\mathbf{v}_l d\mathbf{v}_X, \quad (2)$$

where σ_{lX} is the reaction cross section, $f_l(\mathbf{v}_l)$ and $f_X(\mathbf{v}_X)$ are the density-normalized particle distributions. The function f_X is assumed to be Maxwellian, while f_l is a realistic distribution obtained by solving an appropriate kinetic equation. This method is most accurate and we apply it to neutronic reactions. The realistic neutron distribution is $f_n = f_{n,\mathrm{bulk}} + f_{n,\mathrm{fast}}$, where $f_{n,\mathrm{bulk}}$ is the Maxwellian distribution of bulk neutrons and $f_{n,\mathrm{fast}}$ is the fast neutron distribution function which is related to the fast neutron flux Ψ by $\Psi(E_n) = v_n f_{n,\mathrm{fast}}(E_n)$. The flux satisfies an equation derived in [20]

$$\sum_j n_j \sigma_{tj}^{\mathrm{eff}}(E_n)\Psi(E_n) = \sum_j \int n_j \sigma_{Sj}^{\mathrm{eff}}(E_n' \to E_n)\Psi(E_n')dE_n' + S(E_n). \qquad (3)$$

In Eq. (3), n_j is the number density of background ion species j, $\sigma_{tj}^{\mathrm{eff}}$ is the total cross section for $n - j$ scattering and absorption, $\sigma_{Sj}^{\mathrm{eff}}$ is the differential $n - j$ scattering cross section averaged over the j energy distribution. The term $S = S_{\mathrm{fus}} + S_{\mathrm{upscat}}$ is the fast neutron generation rate. It properly takes into account main sources of fast neutrons, such as fusion reactions (S_{fus}) and close collisions between bulk neutrons and some energetic particles (S_{upscat}).

Let us consider effects caused by nonthermal neutrons (for charged-particle effects, see [16,18]). Reactions having a resonancelike behavior at suprathermal energies and threshold processes are most sensitive to fast neutrons in the plasma. In Table II, these are the resonant $d(n,\gamma)t$ and $^7\mathrm{Be}(n,\alpha)\alpha$ reactions, the endoergic reverse $^3\mathrm{He}(n,d)d$ reaction, and the n-induced breakups of d, $^{6,7}\mathrm{Li}$, and $^7\mathrm{Be}$. Their cross sections (except the $^7\mathrm{Be}$ breakup) are given in [24,25]. The $^7\mathrm{Be}(n,n^3\mathrm{He})\alpha$ cross section can be assumed to be close to the $^7\mathrm{Li}(n,nt)\alpha$ one [17]. The influence of nonthermal neutrons on these processes is demonstrated in Figs. 1–3. Figure 1 presents the ratio of the realistic to Maxwellian rate parameters $\langle\sigma v\rangle/\langle\sigma v\rangle_{\mathrm{M}}$ for the $d(n,\gamma)t$ and $^7\mathrm{Be}(n,\alpha)\alpha$ reactions. The astrophysical rate coefficients $N_{\mathrm{A}}\langle\sigma v\rangle$ and $N_{\mathrm{A}}\langle\sigma v\rangle_{\mathrm{M}}$ for the reverse $^3\mathrm{He}(n,d)d$ reaction are shown in Fig. 2. For comparison, $N_{\mathrm{A}}\langle\sigma v\rangle_{\mathrm{M}}$ for the forward $d(d,n)^3\mathrm{He}$ reaction is also plotted here. The rate coefficients for the n-induced breakups of d, $^7\mathrm{Li}$, and $^7\mathrm{Be}$ are shown in Fig. 3.

Some comments on these figures would be useful here. The reactivity enhancement marked in Fig. 1 results from

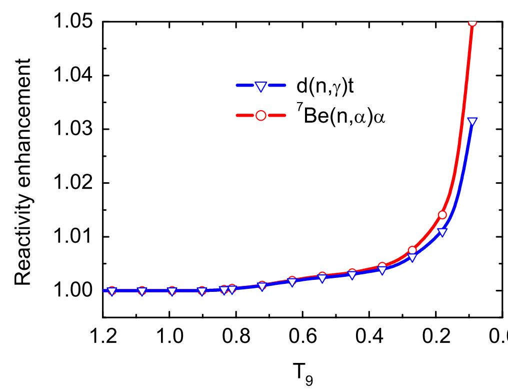

FIG. 1 (color online). The $d(n,\gamma)t$ and $^7\mathrm{Be}(n,\alpha)\alpha$ reactivity enhancement $\langle\sigma v\rangle/\langle\sigma v\rangle_{\mathrm{M}}$ as a function of the Universe temperature.

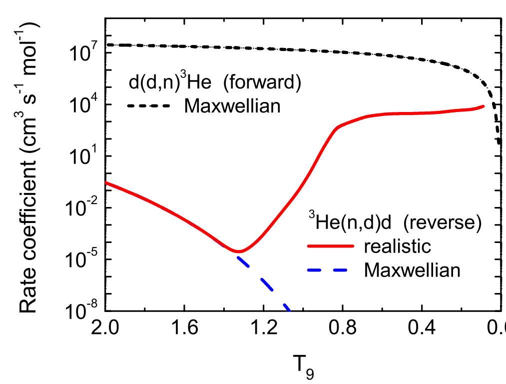

FIG. 2 (color online). The realistic and Maxwellian rate coefficients, $N_{\mathrm{A}}\langle\sigma v\rangle$ and $N_{\mathrm{A}}\langle\sigma v\rangle_{\mathrm{M}}$, for the reverse $^3\mathrm{He}(n,d)d$ reaction. For comparison, $N_{\mathrm{A}}\langle\sigma v\rangle_{\mathrm{M}}$ for the forward $d(d,n)^3\mathrm{He}$ reaction is also shown.

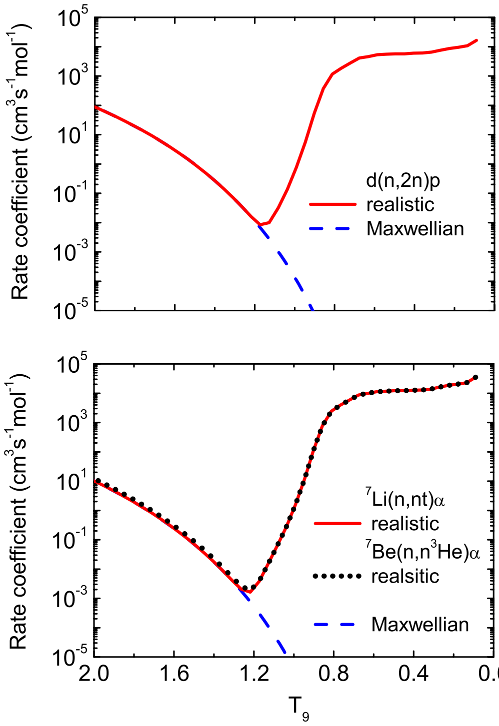

FIG. 3 (color online). The realistic and Maxwellian rate coefficients, $N_A\langle\sigma v\rangle$ and $N_A\langle\sigma v\rangle_M$, for the n-induced breakups of d, ^{7}Li, and ^{7}Be.

reaction resonances at suprathermal energies. The effect, however, is rather weak because the majority of $\langle\sigma v\rangle$ is determined by abundant thermal neutrons, which undergo the reactions with sizable probabilities. At the same time, the nonthermal influence on the endoergic reactions in Figs. 2 and 3 is very strong. These reactions cannot proceed below thresholds and fast neutrons can increase their $\langle\sigma v\rangle$ by orders of magnitude. The effect manifests below some critical temperature $T_{9,\mathrm{cr}} \simeq 1.2$. In this region, the thermal reaction channels are dramatically suppressed and the reactions are maintained by nonthermal neutrons. As a result, the relation between the reverse $n + {}^3\mathrm{He} \rightarrow d + d$ and forward $d + d \rightarrow n + {}^3\mathrm{He}$ reactions departs from the standard law of temperature suppression $\langle\sigma v\rangle_{\mathrm{rev}}/\langle\sigma v\rangle_{\mathrm{forw}} \propto \exp(-Q/T_9)$. To a lesser degree, this effect was also obtained for charged-particle reactions (see, e.g., an analysis of the $p + t \rightleftarrows d + d$ processes [26]).

Now we consider extended BBN simulations allowing for the nonthermal reaction channels shown in Table II. They have been properly incorporated in the standard BBN code [22]. This code has also been updated to work with revised estimates of major thermal nuclear inputs [27] and fundamental constants [28]. The simulations have been done with the WMAP's baryon density $\Omega_B h^2 = 0.02249 \pm 0.00056$ [29] corresponding to a baryon-to-photon ratio of $\eta = (6.16 \pm 0.15) \times 10^{-10}$. In Table III we present the calculated abundances for HHeLi and CNO elements, and indicate their difference δ_{nth} from the thermal BBN predictions due to the nonthermal reaction contribution. For comparison, we also show the thermal abundances change δ_η when η spans the 6.01×10^{-10}–6.31×10^{-10} error range. It is seen that $|\delta_{\mathrm{nth}}| \ll |\delta_\eta|$. The nonthermal corrections for D, ^{4}He, and ^{6}Li prove to be much less than 0.01% and not specified in Table III. The negligible δ_{nth} implies that the nonthermal channels of reactions controlling the abundances of these elements are very weak. For example, the key source of primordial deuterium – the $p(n,\gamma)d$ reaction – is most effective at thermal energies [24] and therefore nonthermal nucleons play here a marginal role. A decrease of the ^{7}Li abundance by 0.02% is mainly caused by new disintegration processes, such as the $^7\mathrm{Be}(n,n^3\mathrm{He})\alpha$ and $^7\mathrm{Li}(n,nt)\alpha$ reactions. Note that this result is in good agreement with other nonthermal calculations, which used a different description of the neutron energy distribution [11] or the ^{7}Be and ^{7}Li

TABLE III. Primordial abundances for HHeLi and CNO elements

Element	Present	δ_{nth} (%)	δ_η (%)	Observation [28]
HHeLi:				
D/H($\times10^{-5}$)	2.529	<0.01	−7.53	2.82 ± 0.21
T/H($\times10^{-8}$)	7.719	0.10	−7.76	
^{3}He/H($\times10^{-5}$)	1.002	−0.01	−2.82	
Y_p($\times10^{-1}$)	2.457	<0.01	0.16	2.49 ± 0.09
^{6}Li/H($\times10^{-14}$)	1.100	<0.01	−7.01	
^{7}Li/H($\times10^{-10}$)	4.474	−0.02	10.78	1.70 ± 0.06 ± 0.44
CNO:				
^{12}C/H($\times10^{-16}$)	6.445	0.59	1.95	
^{13}C/H($\times10^{-16}$)	1.179	0.60	6.88	
^{14}C/H($\times10^{-17}$)	1.125	0.36	12.00	
^{14}N/H($\times10^{-17}$)	4.344	0.53	14.16	
^{15}N/H($\times10^{-20}$)	1.434	0.49	14.33	
^{16}O/H($\times10^{-20}$)	3.027	0.46	17.51	
CNO/H($\times10^{-16}$)	8.171	0.59	3.41	

disintegration rates [17]. One needs to say that the standard CNO network we used is not as advanced as that employed in [9,10]. Therefore, our CNO results are primarily intended to demonstrate how the nonthermal correction may change for elements heavier than HHeLi. Finally, note that the corrections for BeB elements (^{9}Be and ^{10,11}B) are found to be less than 0.01%. Thus, a level of nonthermal effects for the elements with $A \leqslant 16$ does not exceed 0.6%.

III. CONCLUSIONS

In a series of papers [16–18,20] we examined the mechanisms and rates of nonthermal processes naturally triggered in the BBN epoch by fast particles generated in the $t(d, n)\alpha$, $d(d, n)^3$He, $d(d, p)t$, and ^{3}He$(d, p)\alpha$ reactions. The present work follows up these studies, considering the influence of such processes on the primordial element production. The SBBN network has been modified to incorporate the nonthermal events in chain reaction kinetics in the plasma. Totally, $\sim$40 main nonthermal reactions involving nuclei with $A \leqslant 7$ have been allowed for.

It has been recognized that fast neutrons (the most abundant and hot nonthermal plasma species) can effectively maintain some reactions as the Universe cools. For example, at $T_9 \lesssim 1.2$ they appreciably enhance the n-induced breakups of d, ^{7}Li, ^{7}Be, and the ^{3}He$(n, d)d$ reaction as compared with the Maxwellian estimates.

At the same time, however, the nonthermal processes prove to be not strong enough to affect the whole reaction kinetics and essentially change the predictions of thermal BBN. The nonthermal correction to the HHeLi and CNO abundances has been found to be $\leqslant 0.6\%$. The effect could increase if fast particle sources other than the standard reactions would come into play. Such a source—upscattering of bulk neutrons due to collisions with 14.68-MeV protons released in the ^{3}He$(d, p)\alpha$ reaction—was examined in [20]. We found that this mechanism mainly contributes to the production of neutrons of moderate energies $E_n \lesssim 1$ MeV and therefore its role is unlikely to be important. In closing, it seems hardly possible to identify nonthermal mechanisms in standard BBN which could significantly change the element abundances.

[1] R. V. Wagoner, W. A. Fowler, and F. Hoyle, Astrophys. J. **148**, 3 (1967).

[2] R. V. Wagoner, Astrophys. J. Suppl. Ser. **18**, 247 (1969).

[3] D. N. Spergel *et al.*, Astrophys. J. Suppl. Ser. **148**, 175 (2003).

[4] B. D. Fields, Annu. Rev. Nucl. Part. Sci. **61**, 47 (2011).

[5] M. Pospelov and J. Pradler, Annu. Rev. Nucl. Part. Sci. **60**, 539 (2010).

[6] K. Jedamzik and M. Pospelov, New J. Phys. **11**, 105028 (2009).

[7] F. Iocco *et al.*, Phys. Rep. **472**, 1 (2009).

[8] G. Steigman, Annu. Rev. Nucl. Part. Sci. **57**, 463 (2007).

[9] A. Coc, S. Goriely, Yi Xu, M. Saimpert, and E. Vangioni, Astrophys. J. **744**, 158 (2012).

[10] F. Iocco, G. Mangano, G. Miele, O. Pisanti, and P. D. Serpico, Phys. Rev. D **75**, 087304 (2007).

[11] R. N. Boyd, C. R. Brune, G. M. Fuller, and C. J. Smith, Phys. Rev. D **82**, 105005 (2010).

[12] C. J. Smith, G. M. Fuller, and M. S. Smith, Phys. Rev. D **79**, 105001 (2009).

[13] B. Wang, C. A. Bertulani, and A. B. Balantekin, Phys. Rev. C **83**, 018801 (2011).

[14] R. H. Cyburt and M. Pospelov, arXiv:0906.4373.

[15] N. Chakraborty, B. D. Fields, and K. A. Olive, Phys. Rev. D **83**, 063006 (2011).

[16] V. T. Voronchev, Y. Nakao, and M. Nakamura, J. Cosmol. Astropart. Phys. 05 (2008) 010.

[17] V. T. Voronchev, N. Nakamura, and Y. Nakao, J. Cosmol. Astropart. Phys. 05 (2009) 001.

[18] V. T. Voronchev, Y. Nakao, and M. Nakamura, Astrophys. J. **725**, 242 (2010).

[19] M. M. Kang, Y. Hu, H. B. Hu, and S. H. Zhu, arXiv:1110.0163.

[20] Y. Nakao, K. Tsukida, and V. T. Voronchev, Phys. Rev. D **84**, 063016 (2011).

[21] R. V. Wagoner, Astrophys. J. **179**, 343 (1973).

[22] L. Kawano, Report No. FERMILAB-PUB-92/04-A, 1992 (unpublished).

[23] Nonthermal d-induced reactions, such as ^{7}Li$(d, n)2\alpha$ and ^{7}Be$(d, p)2\alpha$, are not considered by us. In SBBN, deuterons are mainly produced in the $p(n, \gamma)d$ radiative capture reaction and therefore do not gain an appreciable energy.

[24] Evaluated Nuclear Data File (ENDF), http://www.nndc.bnl.gov/exfor/endf00.jsp.

[25] Japanese Evaluated Nuclear Data Library (JENDL), http://wwwndc.jaea.go.jp/jendl/j40/j40.html.

[26] V. T. Voronchev, Y. Nakao, and M. Nakamura, J. Phys. G **38**, 015201 (2011).

[27] R. H. Cyburt, Phys. Rev. D **70**, 023505 (2004).

[28] Particle Data Group, K Nakamura *et al.*, J. Phys. G **37**, 075021 (2010).

[29] E. Komatsu *et al.*, Astrophys. J. Suppl. Ser. **192**, 18 (2011).